

1 of 1

94 JS 2
PREPARED FOR THE U.S. DEPARTMENT OF ENERGY,
UNDER CONTRACT DE-AC02-76-CHO-3073

PPPL-2962
UC-420,421,426

PPPL-2962

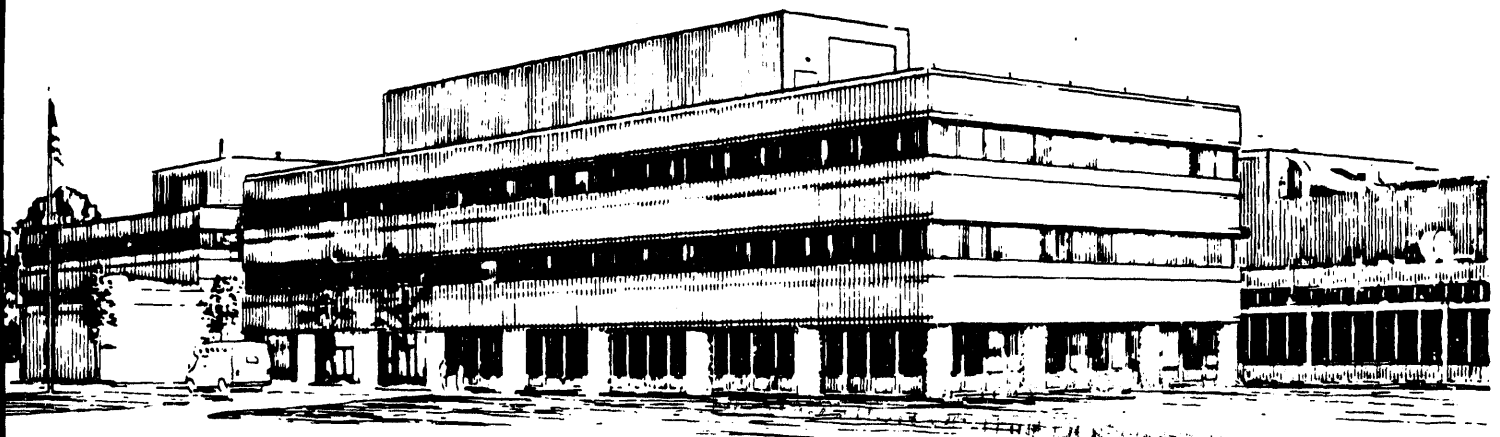
PERFORMANCE OF THE PBX-M PASSIVE PLATE STABILIZATION SYSTEM

BY

H.W. KUGEL, R. BELL, S. BERNABEI, ET AL.

FEBRUARY, 1994

PPPL PRINCETON
PLASMA PHYSICS
LABORATORY



NOTICE

This report was prepared as an account of work sponsored by an agency of the United States Government. Neither the United States Government nor any agency thereof, nor any of their employees, makes any warranty, express or implied, or assumes any legal liability or responsibility for the accuracy, completeness, or usefulness of any information, apparatus, product, or process disclosed, or represents that its use would not infringe privately owned rights. Reference herein to any specific commercial produce, process, or service by trade name, trademark, manufacturer, or otherwise, does not necessarily constitute or imply its endorsement, recommendation, or favoring by the United States Government or any agency thereof. The views and opinions of authors expressed herein do not necessarily state or reflect those of the United States Government or any agency thereof.

NOTICE

This report has been reproduced from the best available copy.
Available in paper copy and microfiche.

Number of pages in this report: 7

DOE and DOE contractors can obtain copies of this report from:

Office of Scientific and Technical Information
P.O. Box 62
Oak Ridge, TN 37831;
(615) 576-8401.

This report is publicly available from the:

National Technical Information Service
Department of Commerce
5285 Port Royal Road
Springfield, Virginia 22161
(703) 487-4650

PERFORMANCE OF THE PBX-M PASSIVE PLATE STABILIZATION SYSTEM

H. W. Kugel, R. Bell, S. Bernabei, T. K. Chu, A. England¹, G. Gettelfinger, R. Hatcher, P. Heitzenroeder, R. Isler¹, S. Jones³, R. Kaita, S. Kaye, B. LeBlanc, M. Ono, M. Okabayshi, N. Sauthoff, L. Schmitz², S. Sesnic, H. Takahashi, W. Tighe, J. Timberlake, S. von Goeler, A. Post-Zwicker¹, and the PBX-M Group.

Princeton Plasma Physics Laboratory, Princeton University, P.O. Box 451, Princeton, NJ 08543

¹Oak Ridge National Laboratory, Oak Ridge, TN 37831

²Institute of Plasma and Fusion Research, UCLA, Los Angeles, CA 90024

³Massachusetts Institute of Technology, MA 02139

ABSTRACT

The PBX-M passive plate stabilization system provides significant stabilization of long-wavelength external kink modes, the slowing of vertical instability growth rates, and the amelioration of disruption characteristics. The passive plate stabilization system has allowed the use of LHCD and IBW to induce current density and pressure profile modifications, and $m=1$ divertor biasing for modifying edge plasma transport. Improvements in the passive plate system insulators and support structures have provided reliable operation. Impurity influxes with the close-fitting passive plates are low. Solid target boronization is applied routinely to reduce conditioning time and maintain clean conditions.

INTRODUCTION

A strong cross-sectional indentation is applied to obtain bean-shaped plasmas for controlling magnetic curvature and shear. Active control of current and pressure profiles is performed using LHCD, pellet injection, IBW heating, and neutral beam injection. An electrically isolated, close-fitting, conducting, passive plate shell, with toroidal and poloidal gaps, surrounds over 70% of the plasma and provides stabilization of long-wavelength external kink modes, ameliorates disruption characteristics, and slows the growth rates of vertical instabilities. Feedback systems incorporating these features and possible synergies with the profile control techniques are under investigation as candidates for active control of disruption. PBX-M high- β and profile modification experiments for accessing the near second stability regime have been discussed previously [1-3]. In this work, we review some aspects of the improved control, disruption, and operational characteristics that accrue from the passive plate stabilization system.

II. SYSTEM DESCRIPTION

Fig.1 shows internal hardware details of the passive plates system, internal coils, poloidal limiters, and internal buses and insulating shields for passive plate biasing experiments. The passive plates stabilization system is comprised of 5 pairs of electrically isolated, single-turn plates, positioned above and below the magnetic axis. The plates consist of 2.5 cm thick aluminum (6061-T6) clad with a 0.3 cm thick layer of explosively bonded stainless steel (304-SS). The final configuration was achieved by bolting

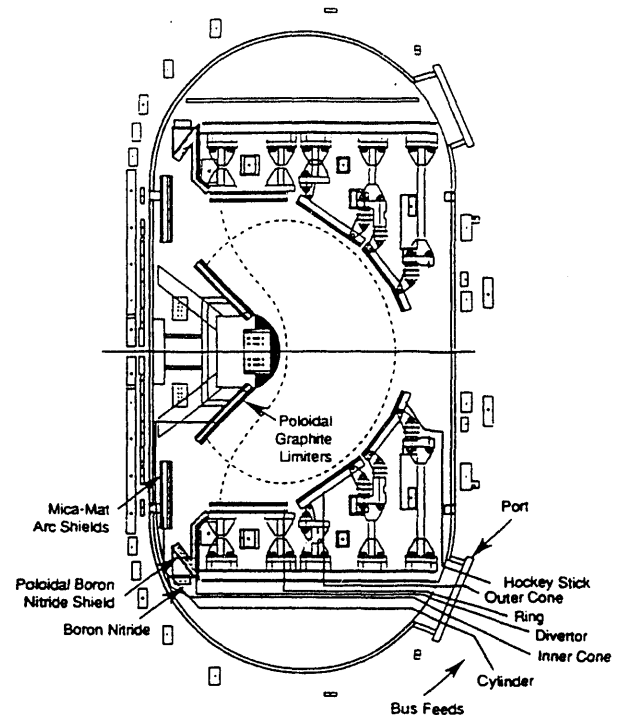


Fig.1 Partial schematic showing internal hardware.

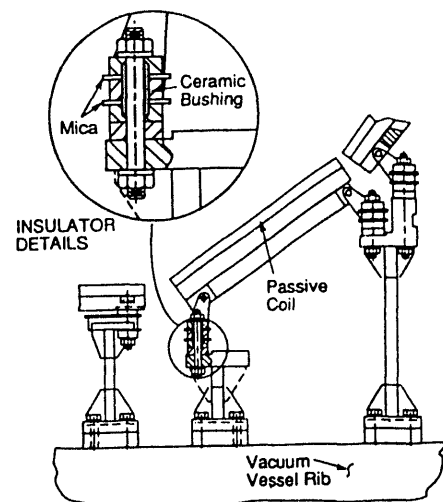


Fig. 2 Partial schematic showing details of passive plate support system.

MASTER

EP

III. PLASMA PERFORMANCE

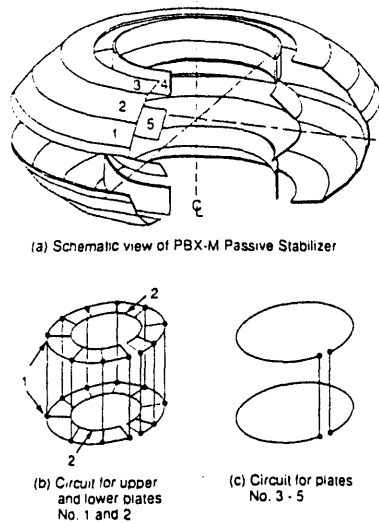


Fig.3 Schematic of passive plate elements and connections.

together 70 individual segments, each small enough to pass through a vessel port. The bolted segments were fastened with nickel-plated splice plates. Insulated bridge plates provided mechanical continuity across toroidal gaps in each plate. Shown in Fig. 1 are the locations of the 2 cm high ATJ graphite poloidal limiters located on the passive plates at 12 toroidal locations. The passive plate system is designed to preclude interference with 17 interior water-cooled magnetic coils, 4 NBI ducts, 2 IBW heating antennas, 2 LHCD couplers, and various diagnostic assemblies.

Fig. 2 is a schematic diagram showing details of the support system and electrical insulators[4]. The electrical isolation requirements are achieved using over 400 ceramic alumina insulators together with about 42 m² of mica sheet for associated shields. The five elements of the passive plate system (Fig.3a) are separated from each other with a poloidal gap, and each plate has a toroidal gap to provide the requisite OH electrical isolation. Fig. 3b shows the present electrical connection of top and bottom plate pairs in a saddle coil arrangement. Plates of the two outer pairs (1-2), are connected to each other and also upper-to-lower. The upper-to-lower connection is accomplished by vertical nickel-plated aluminum buses at 11 locations. These connections facilitate the flow of eddy currents and reduce the effect of the 40 cm mid-plane gap required for auxiliary heating, and diagnostic access. The upper and lower plates of the three inner pairs are connected electrically via buses at one location (Fig.3b). The outer two pairs, designated "Hockey-Stick"(1) and "Outer-Cone"(2), act to stabilize primarily n=1 external kink modes. The three inner pairs, designated "Ring"(3), "Cylinder"(4), and "Inner-Cone"(5), perform stabilization of the n=0 vertical modes. The passive plate diagnostics are Rogowski coils on the vertical buses shown in Fig.3b, and segmented loops embedded in the front surfaces of the plates. Other nearby in-vessel diagnostics include single-turn flux loops, thermocouples, divertor pressure gauges, and a diamagnetic loop. This in-vessel instrumentation requires about 2 km of interior instrumentation wiring with various types of electrical, thermal, and electromagnetic insulation.

The three inner pairs of passive plates (3-5), perform stabilization of the n=0 vertical modes. Previous work has shown that, with the vertical position feedback system disabled, the passive plates provided vertical stabilization to the plasma, for about 50 msec, before the plasma began moving vertically with an initial velocity of about 133 cm/s [5,6]. This ample duration of vertical stability allows the active feedback system to dampen vertical instabilities. Recent performance of this system is discussed elsewhere in this conference [7].

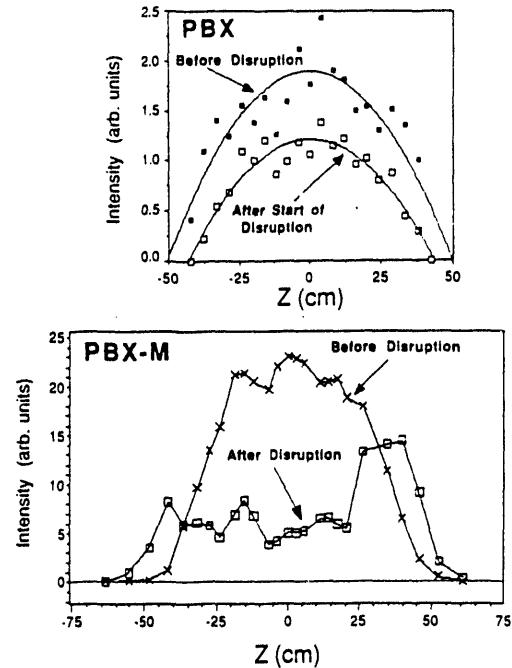


Fig. 4 The character of disruptions is different in PBX-M and PBX.

Fig.4 shows that the character of disruptions in PBX-M differs from that of the predecessor PBX which had more distant passive plates [1]. Chord-averaged soft x-ray (SXR) signals show that the collapse of the central region occurs across the entire profile to the edge in PBX, whereas in PBX-M, edge confinement is maintained for about 100 msec after the central collapse. This behavior implies that, due to the "tight-coupling" of the passive plates, internal processes, rather than external edge effects, are the primary cause of PBX-M disruptions[1].

Another effect of the passive plates can be seen in Fig. 5 which compares the PBX-M precursor duration times for indented, bean-shaped, "tightly-coupled" discharges with those for nearly circular, "loosely coupled" discharges. The significantly slower growth times for the "tightly-coupled" discharges may allow the use of active disruption avoidance control [8]. Plasma current decay rates following disruption depend on profile shape [9].

Lower Hybrid Current Drive (LHCD) has been applied to significantly modify PBX-M current density profiles in the presence of the closely-coupled passive plate stabilization system [3]. LHCD of frequency 4.6 GHz and powers up to 600 kW has been applied with a fast response

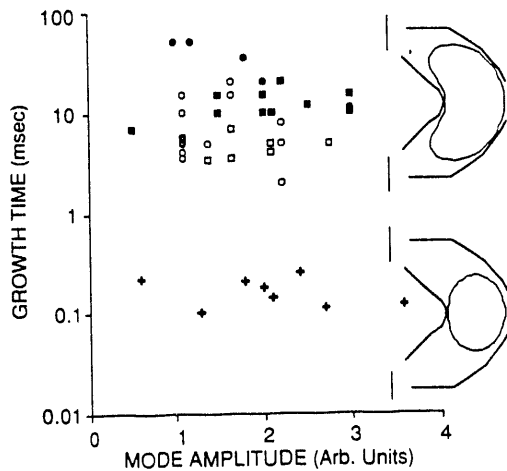


Fig. 5 Disruption precursor times are longer for close-coupling (top) and shorter for loose-coupling (bottom).

phase shifter which adjusts the phase of the launched wave during the discharge. A total power of 2 MW is planned using the 2 launchers each coupled to 32 wave guides. Fig. 6 shows the time evolution of the hard x-ray intensity for an indented plasma with LHCD and NBI along a vertical cord through the magnetic axis. The emission profile became hollow and the $q=1$ profile decreased with the application of LHCD [3,10].

Ion Bernstein wave heating (IBW) has been applied to significantly modify PBX-M pressure profiles and provided localized bulk ion heating in the presence of the closely-coupled passive plate stabilization system [3,11]. The 2 MW IBW system with operating frequencies in the range from 40 to 80 MHz uses two antennae. Fig. 7 shows peaked density profiles with IBW for shaped plasmas. It is seen that in strongly heated, bean-shaped discharges, a peaked density profile evolves during the late phase of IBW injection from a flat H-mode-like density profile [3, 11].

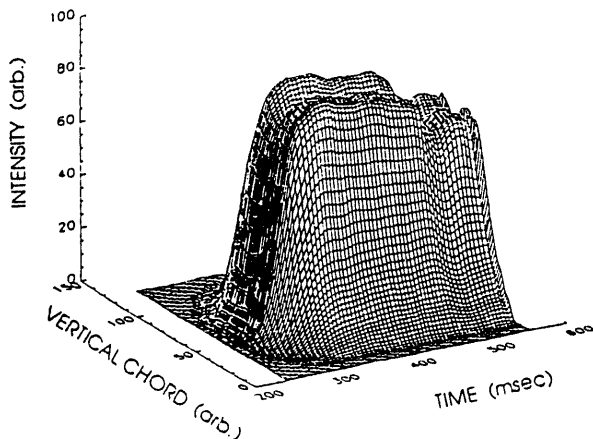


Fig. 6 Time evolution of the intensity of hard x-rays along a vertical cord during applied LHCD.

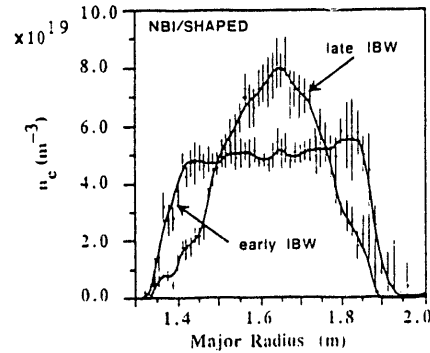


Fig.7 Peaked density profiles with IBW.

Edge plasma transport was modified using divertor biasing [3, 14]. Preliminary, $m=1$ divertor biasing experiments have been applied to PBX-M using the passive plate buses shown in Fig.3. Bias voltages $-75 \text{ V} \leq V_b \leq 75 \text{ V}$ were applied to the Inner Cone (2) and Ring (3) passive plate elements and bias currents of $-300 \text{ A} < I_b < 200 \text{ A}$ were observed. Fig. 8 shows the NBI power required to achieve H-modes was lowered 25% with the application of edge biasing voltages $> 25 \text{ V}$. Biasing experiments at higher voltages and currents, and other configurations are planned to make use of the versatility offered by the passive plate system.

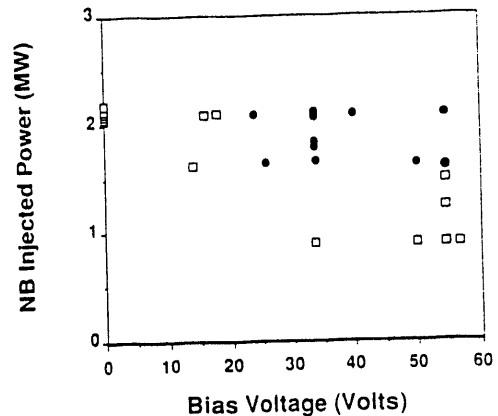


Fig. 8 Initial $m=1$ divertor biasing lowered H-mode NBI power threshold by 25%. The solid symbols correspond to H-mode discharges; open symbols correspond to L-mode discharges.

IV. OPERATING PERFORMANCE

Damage occurred in 1988 during the initial testing of the passive plate system, and was attributed to the single-point grounding of each individual plate to the vacuum vessel, the use of organic insulators in some locations, and arcing between support structures along toroidal field lines [4]. High power operations with the present configuration, described previously [4], have not encountered these difficulties.

Initially, single-point grounding of each passive plate was employed [4]. This allowed the halo plasma to form closed circuit paths for large current flows through the

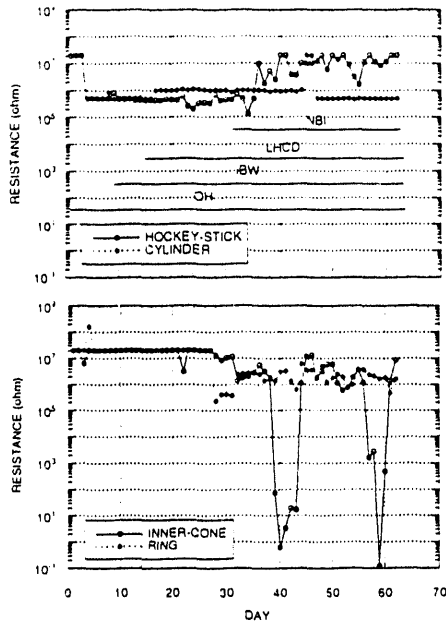


Fig.9 Passive plate resistance to vessel-ground varies. Impurity deposition during high power operation lowers the resistance of divertor region insulators.

supports and the vessel. These currents caused severe damage to mechanical supports. This effect was eliminated to date by connecting each passive plate element to vessel-ground through an external, 500 Ω carbon resistor. This limits current flows, and maintains plate potential relative to vessel-ground.

The previous use of organic (polyimide) insulators in some locations resulted in nitrogen pressure bursts during operations [4]. These pressure bursts are believed to be the result of arcing across the organic insulators during transients which would char the surface and irreversibly damaged the organic insulators. This was eliminated by replacing all organic insulators with alumina insulators and eliminating all direct-line-of-sight arc paths.

Arcing along toroidal flux lines, between support structures nominally at the same potential, was greatly reduced using shields fabricated from mica-mat [4]. Some discoloration from such arcing still is observed at some locations, but the residual arcing has not been sufficient to cause significant damage, out-gassing, or other operation difficulties.

Prior to daily operations, the 500 Ω drain resistors are disconnected, and the resistance between each passive plate and vessel-ground is measured in both polarity directions. The electrical isolation of the passive plates, as measured with a standard 9 v ohmmeter, are found to undergo daily variations. Fig. 9 shows typical results of these daily measurements. The largest changes occur during high power operation for passive plates located in the divertor region. This may be due to the preferential power and impurity depositions received by these passive plates from the strike points and disruptions [9]. Higher voltage resistance measurements to help identify the nature of these conducting paths have been avoided so as not to introduce possibly irreversible breakdown damage.

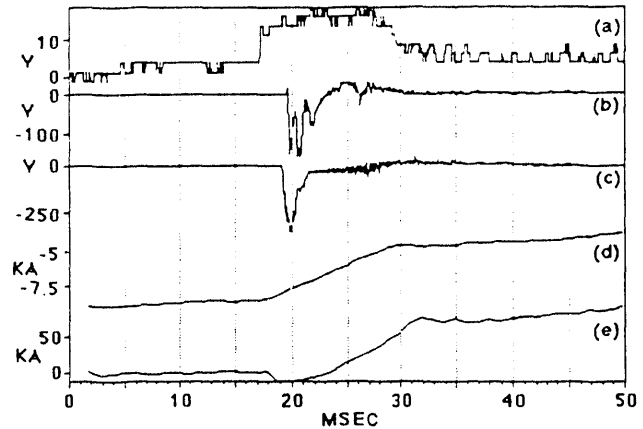


Fig.10 Passive plate voltage waveforms at startup of 400 kA discharge for (a) passive plate No.5 toroidal gap, (b) the poloidal gap between plates No.2 and No.3, (c) an outer poloidal limiter relative to plate No.1, (d) ohmic current, and (e) plasma current

However, after several vessel vents, these conducting and sometimes semiconducting paths undergo chemical changes and become insulating. This behavior suggests that these impurity films could not support large current flows between the plasma and vessel-ground. The presence of these films during operations has not produced any degradation in performance.

The initial measurements found that the largest induced voltages were observed at plasma startup and at plasma current disruption and exhibited characteristics depending on the operating conditions. Fig. 10 and 11 show typical passive plate waveforms at startup and disruption, respectively. The highest voltages observed have been at disruption and were less than 2 kV [12].

The issue of the proximity of the edge plasma to the passive plate surface, the resultant impurity influxes, and consequent radiation were early concerns. The radiated power was highest at the edge and only mildly peaked on the plasma center in highly indented, high- β_t discharges, with the plasma closest to the plates [14]. Typical central plasma

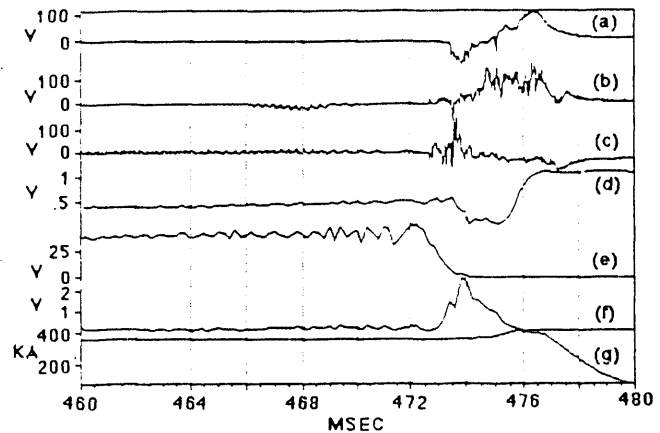


Fig. 11 Passive plate voltage waveforms at disruption for a 400 kA discharge for (a) passive plate No. 5 toroidal gap, (b) passive plate No.2-No.3 poloidal gap, (c) an outer poloidal limiter relative to passive plate No.1, (d) a segmented flux loop difference, (e) a central soft x-ray detector, (f) an outer soft x-ray detector, and (g) the plasma current.

EXTERNAL DISTRIBUTION IN ADDITION TO UC-420

Dr. F. Paoloni, Univ. of Wollongong, AUSTRALIA
 Prof. M.H. Brennan, Univ. of Sydney, AUSTRALIA
 Plasma Research Lab., Australian Nat. Univ., AUSTRALIA
 Prof. I.R. Jones, Flinders Univ, AUSTRALIA
 Prof. F. Cap, Inst. for Theoretical Physics, AUSTRIA
 Prof. M. Heindler, Institut für Theoretische Physik, AUSTRIA
 Prof. M. Goossens, Astronomisch Instituut, BELGIUM
 Ecole Royale Militaire, Lab. de Phy. Plasmas, BELGIUM
 Commission-European, DG. XII-Fusion Prog., BELGIUM
 Prof. R. Bouciqué, Rijksuniversiteit Gent, BELGIUM
 Dr. P.H. Sakanaka, Instituto Fisica, BRAZIL
 Prof. Dr. I.C. Nascimento, Instituto Fisica, Sao Paulo, BRAZIL
 Instituto Nacional De Pesquisas Espaciais-INPE, BRAZIL
 Documents Office, Atomic Energy of Canada Ltd., CANADA
 Ms. M. Morin, CCFW/Tokamak de Varennes, CANADA
 Dr. M.P. Bachynski, MPB Technologies, Inc., CANADA
 Dr. H.M. Skarsgard, Univ. of Saskatchewan, CANADA
 Prof. J. Teichmann, Univ. of Montreal, CANADA
 Prof. S.R. Sreenivasan, Univ. of Calgary, CANADA
 Prof. T.W. Johnston, INRS-Energie, CANADA
 Dr. R. Bolton, Centre canadien de fusion magnétique, CANADA
 Dr. C.R. James,, Univ. of Alberta, CANADA
 Dr. P. Lukác, Komenského Universzita, CZECHO-SLOVAKIA
 The Librarian, Culham Laboratory, ENGLAND
 Library, R61, Rutherford Appleton Laboratory, ENGLAND
 Mrs. S.A. Hutchinson, JET Library, ENGLAND
 Dr. S.C. Sharma, Univ. of South Pacific, FIJI ISLANDS
 P. Mähönen, Univ. of Helsinki, FINLAND
 Prof. M.N. Bussac, Ecole Polytechnique,, FRANCE
 C. Mouttet, Lab. de Physique des Milieux Ionisés, FRANCE
 J. Radet, GEN/CADARACHE - Bat 506, FRANCE
 Prof. E. Economou, Univ. of Crete, GREECE
 Ms. C. Rinni, Univ. of Ioannina, GREECE
 Preprint Library, Hungarian Academy of Sci., HUNGARY
 Dr. B. DasGupta, Saha Inst. of Nuclear Physics, INDIA
 Dr. P. Kaw, Inst. for Plasma Research, INDIA
 Dr. P. Rosenau, Israel Inst. of Technology, ISRAEL
 Librarian, International Center for Theo Physics, ITALY
 Miss C. De Palo, Associazione EURATOM-ENEA , ITALY
 Dr. G. Grosso, Istituto di Fisica del Plasma, ITALY
 Prof. G. Rostangni, Istituto Gas Ionizzati Del Cnr, ITALY
 Dr. H. Yamato, Toshiba Res & Devel Center, JAPAN
 Prof. I. Kawakami, Hiroshima Univ., JAPAN
 Prof. K. Nishikawa, Hiroshima Univ., JAPAN
 Librarian, Naka Fusion Research Establishment, JAERI, JAPAN
 Director, Japan Atomic Energy Research Inst., JAPAN
 Prof. S. Itoh, Kyushu Univ., JAPAN
 Research Info. Ctr., National Instit. for Fusion Science, JAPAN
 Prof. S. Tanaka, Kyoto Univ., JAPAN
 Library, Kyoto Univ., JAPAN
 Prof. N. Inoue, Univ. of Tokyo, JAPAN
 Secretary, Plasma Section, Electrotechnical Lab., JAPAN
 S. Mori, Technical Advisor, JAERI, JAPAN
 Dr. O. Mitarai, Kumamoto Inst. of Technology, JAPAN
 Dr. G.S. Lee, Korea Basic Sci. Ctr., KOREA
 J. Hyeon-Sook, Korea Atomic Energy Research Inst., KOREA
 D.I. Choi, The Korea Adv. Inst. of Sci. & Tech., KOREA
 Prof. B.S. Liley, Univ. of Waikato, NEW ZEALAND
 Inst of Physics, Chinese Acad Sci PEOPLE'S REP. OF CHINA
 Library, Inst. of Plasma Physics, PEOPLE'S REP. OF CHINA
 Tsinghua Univ. Library, PEOPLE'S REPUBLIC OF CHINA
 Z. Li, S.W. Inst Physics, PEOPLE'S REPUBLIC OF CHINA
 Prof. J.A.C. Cabral, Instituto Superior Tecnico, PORTUGAL
 Prof. M.A. Hellberg, Univ. of Natal, S. AFRICA
 Prof. D.E. Kim, Pohang Inst. of Sci. & Tech., SO. KOREA
 Prof. C.I.E.M.A.T, Fusion Division Library, SPAIN
 Dr. L. Stenflo, Univ. of UMEA, SWEDEN
 Library, Royal Inst. of Technology, SWEDEN
 Prof. H. Wilhelmson, Chalmers Univ. of Tech., SWEDEN
 Centre Phys. Des Plasmas, Ecole Polytech, SWITZERLAND
 Bibliotheek, Inst. Voor Plasma-Fysica, THE NETHERLANDS
 Asst. Prof. Dr. S. Cakir, Middle East Tech. Univ., TURKEY
 Dr. V.A. Glukhikh, Sci. Res. Inst. Electrophys. I Apparatus, USSR
 Dr. D.D. Ryutov, Siberian Branch of Academy of Sci., USSR
 Dr. G.A. Eliseev, I.V. Kurchatov Inst., USSR
 Librarian, The Ukr.SSR Academy of Sciences, USSR
 Dr. L.M. Kovrizhnykh, Inst. of General Physics, USSR
 Kernforschungsanlage GmbH, Zentralbibliothek, W. GERMANY
 Bibliothek, Inst. Für Plasmaforschung, W. GERMANY
 Prof. K. Schindler, Ruhr-Universität Bochum, W. GERMANY
 Dr. F. Wagner, (ASDEX), Max-Planck-Institut, W. GERMANY
 Librarian, Max-Planck-Institut, W. GERMANY

**DATE
FILMED**

3 / 23 / 94

END

